COMPRESSION OF IMAGE DATA FROM REMOTE SENSING SATELLITES

J.Cl. Degavre
European Space Research & Technology Centre
Noordwijk, The Netherlands
Comission II

Abstract

A summary is presented of the results obtained by the European Space Research & Technology Centre (ESTEC) from its experiments of the compression on remote sensing satellites image data. Examples of the required instrumentation are given for both on-board satellite and ground applications.

1. INTRODUCTION

The successful utilization of image data from remote sensing satellites has stimulated the development of imaging sensors. The technology will satisfy the user's desire for finer spatial and spectral resolution. Forecasts suggest that 10m spatial resolution and 20nm spectral resolution design goals will be met in the next few years [1, 2]. The new data rate generated by such sensors will reach several gegabits per second and will exceed the planned data relay satellites capability. Efficient encoding, or data compression, in combination with the selection in flight of subsets of the imaging sensor capabilities will be mandatory.
As part of its on-board satellite signal processing technology programme, the European Space Research and Technology Centre (ESTEC) has conducted several studies on the design of image data compression algorithms suitable for remote sensing image data. An algorithm has been selected and tested extensively on satellite imagery.

2. THE COMPRESSION ALGORITHM

A compression algorithm has been developed at ESTEC by D. Chaturvedi [3] It consists in quantizing and encoding the image data after Cosine Transformation. The transformation, quantization and encoding are performed, block by block, over the complete image scan. The block is typically a square of 16x16 pixels.

After Cosine Transformation, the data are much less correlated than the initial image grey levels and can be coded with less redundancy. Because natural images tend to have decreasing energy versus increasing spatial frequencies, the quantized data in the Cosine Domain can be pre-arranged in order of decreasing word length and coded with an efficient variable word length encoding scheme. The word length of each Cosine Transformed data sample depends of its amplitude and of the selected quantization step. The image is reconstructed by reversing all the operations after the word synchronisation has been recovered from the auxiliary data.
The functional block diagram of the compressor/decompressor is shown on fig. 1. The compression ratio obtained varies from block to block and is a function of the image spatial frequency content.

2.1 Theoretical Performance

As the quantization of the Cosine Transformed image data samples is performed with uniform step and since the transformation is unitary, the mean squared difference between the original image and the image reconstructed after compression and decompression is given by the

expression of the noise power generated by the uniform quantizer, i.e.

$$\text{mean squared error} = \frac{Q^2}{12}$$

where Q is the quantization step.

The quantization error on each Cosine Transformed data sample are independent and uniformaly distributed between -Q/2 and +Q/2. The mean image reconstruction error is zero, so that no biasing is introduced by the compression.

The distribution of the errors on the image pixels reconstructed by Inverse Cosine Transformation is given by the Central Limit Theorem. This theorem states that, under rather general conditions, the linear combination of a large number of random variables has, at the limit a Gaussian distribution.

The Inverse Cosine Transformation performed by the compressor constituting a linear operation performed on a block of 256 quantized data samples, the error on the reconstructed image can be approximated as Gaussian and the probability of an error of X grey tone units will be given by the expression:

$$p(X) = \frac{\sqrt{12}}{Q\sqrt{2\pi}} \int_{X-\frac{1}{2}}^{X+\frac{1}{2}} \exp\left(-6x^2/Q^2\right)dx$$

The peak image coding error can be considered, for all practical purposes, as, say, the error not exceeded by more than one pixel every million. The expression of the peak error, derived from the cumulative Gaussian distribution, is then: peak error = [2Q] where [x] denotes the nearest integer value to x.

The reconstruction error is thus controlable by setting the corresponding value of Q. When Q is selected, the image reconstruction distortion is fixed. The compressor is then operating in "constant distortion mode". The distortion can be made as low as desirable, and in particular, inferior to the sensor quantization noise level. Only the arithmetic noise generated by the digital machine performing the Cosine Transformation prevents the compression with full reversibility.

By varying the image reconstruction error from block to block, the compressor can operate in "fixed compression mode". This implies compressing the image block in two steps. In the first step the compression ratio obtained withe the current value of Q is calculated. In the second step, a new value of Q is determined, using the logarithmic relationship between data rate and distortion error, allowing to encode the data with the number of bits available.

The minimum number of bits R required to transmit uniformly quantized single sample Gaussian random data with a mean squared distortion D is given by the expression [4]:

$$R(D) = 0.25 + 0.5 \log \frac{S}{D}$$

where S is the standard deviation of the data.

The performance of an encoding scheme can be tested by compressing random Gaussian image and comparing the number of bits required as a function of the error tolerated. Figure 2 shows the Chaturvedi's algorithm performance. The test image was generated by a two-dimensional autoregressive process giving the Gaussian Markov random field:

$$I(i,j) : \rho_1 I(i-1,j) + \rho_2 I(i,j-1) - \rho_1 \rho_2 I(i-1,j-1) + Wij$$

where Wij is a zero mean Gaussian sequence with standard deviation S and ρ_1, ρ_2 the horizontal and vertical correlation of the image. It can be seen that the coding performance is almost independent of the spatial correlation, as the Cosine transformation decorrelates the data prior to quantization and encoding. The overall algorithm performance is approximately 0.75 bits away from the theoretical bound.

2.2 Performance on Earth Remote Sensing Satellite Image Data

The Chaturvedi's compression algorithm has been experimented on multispectral images received from Meteosat (visible, infra-red and water vapour channels), Nimbus 7 (CZCS, 7 channels) and Landsat 3 (MSS, 4 channels). For each sensor, the spectral channels were coded separately. The results are plotted on figure 3, indicating the average number of bits per pixel required to encode the different satellite images as a function of the tolerated average reconstruction error, expressed in grey tone units. It can be seen how the information content of the image differ from sensor to sensor.

The apparent activity of the raw Meteosat Water Vapour image is due to the sensor noise present. It indicates the necessity of noise filtering before efficiently encoding the image.

Figures 4a and 4b indicate the average number of bits required to encode the four types of images considered when 98 to 99% of the image must be reconstructed without error, or with an accuracy of one grey tone unit or with an accuracy of two grey tone units.
One can see, for example, that for a reconstruction accuracy of one grey tone unit, 3.7 bits per pixel are required to encode the Landsat scene, while 2.7 bits are sufficient, if an accuracy of two grey tone units is tolerated.

Measured absolute peak errors are given in the table of figure 5 together with the theoretical values derived in the previous section.

To give a better feeling of the performance of the compression algorithm let us, for example, express the typical transmission link bit error of 10^{-5} in equivalent image error. For an 8 bits image data, the average mean squared error caused by the transmission error is:

$$\text{equivalent rms error} = 10^{-5} (1 + 2^2 + 4^4 + \ldots + 128^2) = 0.46$$

If a comparable error is tolerated for image encoding, a substantial compression ratio is obtained with a peak reconstruction error of 2 grey tone units whereas transmission error can cause an error as high as 128 grey tone units if the most significant bit is affected.
The photographs reproduced at the end of the article show parts of the original test scenes (top left corner), of the reconstructed scenes (bottom right corner), of the image of difference or reconstruction noise with its superposed histogram (bottom left corner) and of the image of the

difference amplified 16 times (top right corner). Zero error is presented by the mid grey tone. One can verify on the image of the reconstruction error that no image feature is apparent.

3. THE COMPRESSION/DECOMPRESSION INSTRUMENTATION

The image data encoder can be placed at different points of the end to end Satellite Remote Sensing data system. Depending of its location, encoding provides different advantages:

- The amount of raw data acquired in real time through a given transmission link bandwidth increases if an encoder is placed at the image sensor output.
- The amount of acquired play-back data, and consequently the coverage of the mission, increases, for a given on-board mass storage capacity if the image data is encoded before storing. The stored data can be decompressed prior to transmission if a transparent system is desired.
- The amount of play-back data acquired by the receiver during the satellite visibility period increases if compressed data is recorded and compressed data transmitted.
- The amount of data archived or the archiving period can be increased if the data is encoded.
  The image can be reconstructed when retreived or after it has been disseminated.
- The time required to disseminate archived data is reduced if the data is coded.
  The coding algorithm must then be imposed as a standard, and the user receiver must be equiped with the corresponding decoder.

The "National Aerospace Laboratory" (NLR, Netherlands) is developing for the European Space Research and Technology Centre (ESTEC) a prototype model, also called elegant breadboard, of a micro-programmed image processor, adapted to the Chaturvedi image encoding/decoding algorithm. The objective of the development is to demonstrate the feasibility of on-board satellite image compression/decompression at high throughput rate with a relative low power consumption. The breadboard will be able to compress/decompress an image of 2048 pixels per line, originally coded with 8 bits per pixel, at a line rate of 300 lines per second (input data rate = 4.8 Mbits/sec). The total power consumption of the breadboard will approximately be 12 Watts. Its weight will be about 8 Kg. ESTEC is also engaged with the firms MATRA (F) and SAAB (S) on the development of a so-called "High Speed Programmable On-board Processor" designed with a high degree of general purposeness and modularity [6], [7]. Its architecture features result from the study of a wide range of on-board image processing applications like radiometric calibration, image compression, Synthetic aperture radar signal processing, etc. The processor has a multibus structure designed to federate the processor devices that are appearing on the communication and military markets. Emphasis has been put on the definition of the bus protocol and the synchronisation mechanisms. Each bus has a throughput of 10 Mbits/sec. A standard circuit, to be large scale integrated, interfaces each processing element to two busses. It is foreseen, later this year, to implement the Chaturvedi's algorithm on the High Speed Programmable Processor breadboard.

A ground-based version of the compressor/decompressor can be derived from its on-board implementation. Prototypes of on-board versions could, for example, be used.

An all-software implementation of the Chaturvedi algorithm on a general purpose computer, part of a typical ground station instrumentation, can also be interesting. As an indication, ESTEC has implemented a 1 line per second (2048 pixels per line) compressor/decompressor on a VAX 11/750 computer augmented by an AP 120/B array processor, using standard library routines.

4. CONCLUSIONS

It is possible to compress image data from Remote Sensing Satellites to an average of 2 to 3 bits per pixel with an image reconstruction accuracy commensurable with the sensor thermal noise, the sensor quantizer noise or the transmittion noise present on the data.

With the compression algorithm tested, pictorial degradation becomes visible when coding with an average of about one bit per pixel. At that stage, only tests on the quality of the thematic end user product can tell if the degradation is acceptable.
Compressors/decompressors for use on-board the satellite are under development.

References

[1] "Trends in Solid State Image Sensors for Remote Sensing". J.L. Lowrance, Princeton University Observatory - Princeton N.J.08544 1982 Geoscience and Remote Sensing Symposium WP-2, p. 2.1.

[2] "An Advanced Multispectral Imaging Concept". J.B. Wellman et al. J.P.L. California Institute of Technology - 1982 Geoscience and Remote Sensing Symposium WP-2, p. 4.1.

[3] "Three Image Compression Algorithms". D. Chaturvedi, European Space Research & Technology Centre - Noordwijk (NL). Internal note THA/DC/1177/av - July 1983.

[4] "Analog source digitization: A comparison of Theory and Practice", T.J. Goblick, J.L. Holsinger, IEEE Trans. Inform. Theory, Vol. IT-13, pp. 323-326, April 1967.

[5] "Some Design Considerations on a Fast Reliable and low-power Multi-Processor System for Image Processing on-board Scientific Satellites". F.A. Gerritsen, A. Monkel, H.F.A. Roefs - National Aerospace Laboratory (NLR) - The Netherlands, Ref. NLR MP83071U.

[6] "The Design of a Parallel Processor for Image Processing On-Board Satellites": An Application Oriented Approach. G. Gaillat - MATRA 10th Annual Symposium on Computer Architecture, Stockholm , June 13-16, 1983.

[7] "Study of a Programmable High Speed Processor for Use On-board Satellites". J.Cl. Degavre et al. AIAA Computers in Aerospace Conference , October 22-26, 1983 - Hartford, Connecticut.

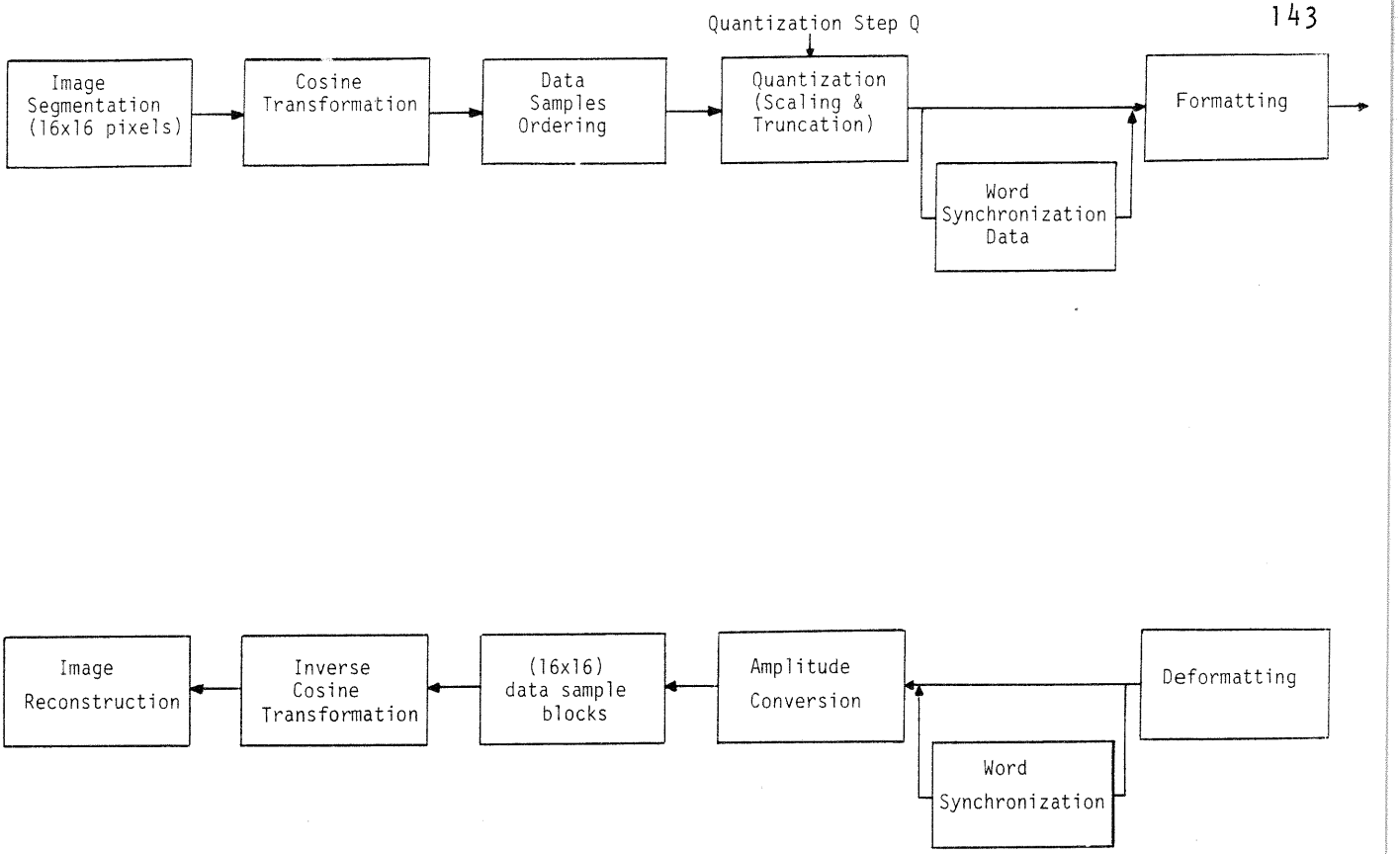

Figure 1 - Chaturvedi Algorithm block diagram

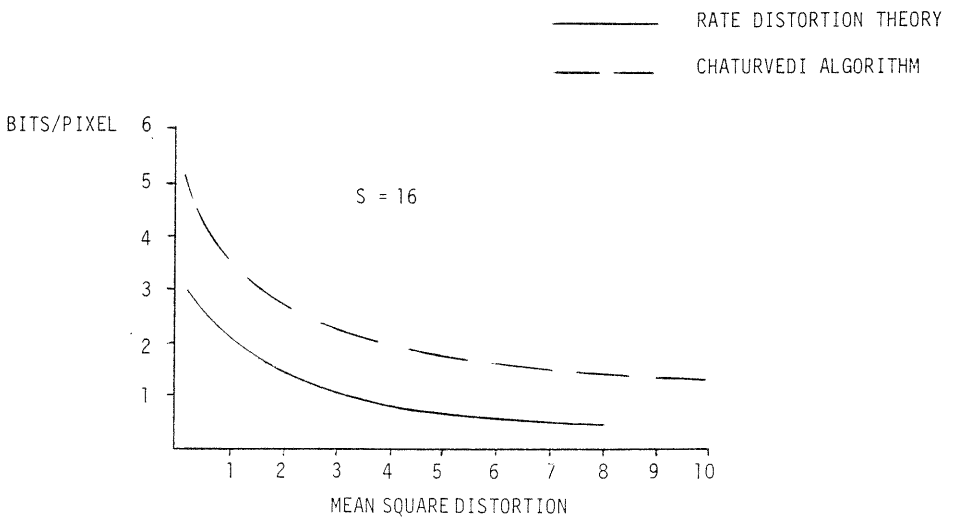

Figure 2 - Theoretical Performance

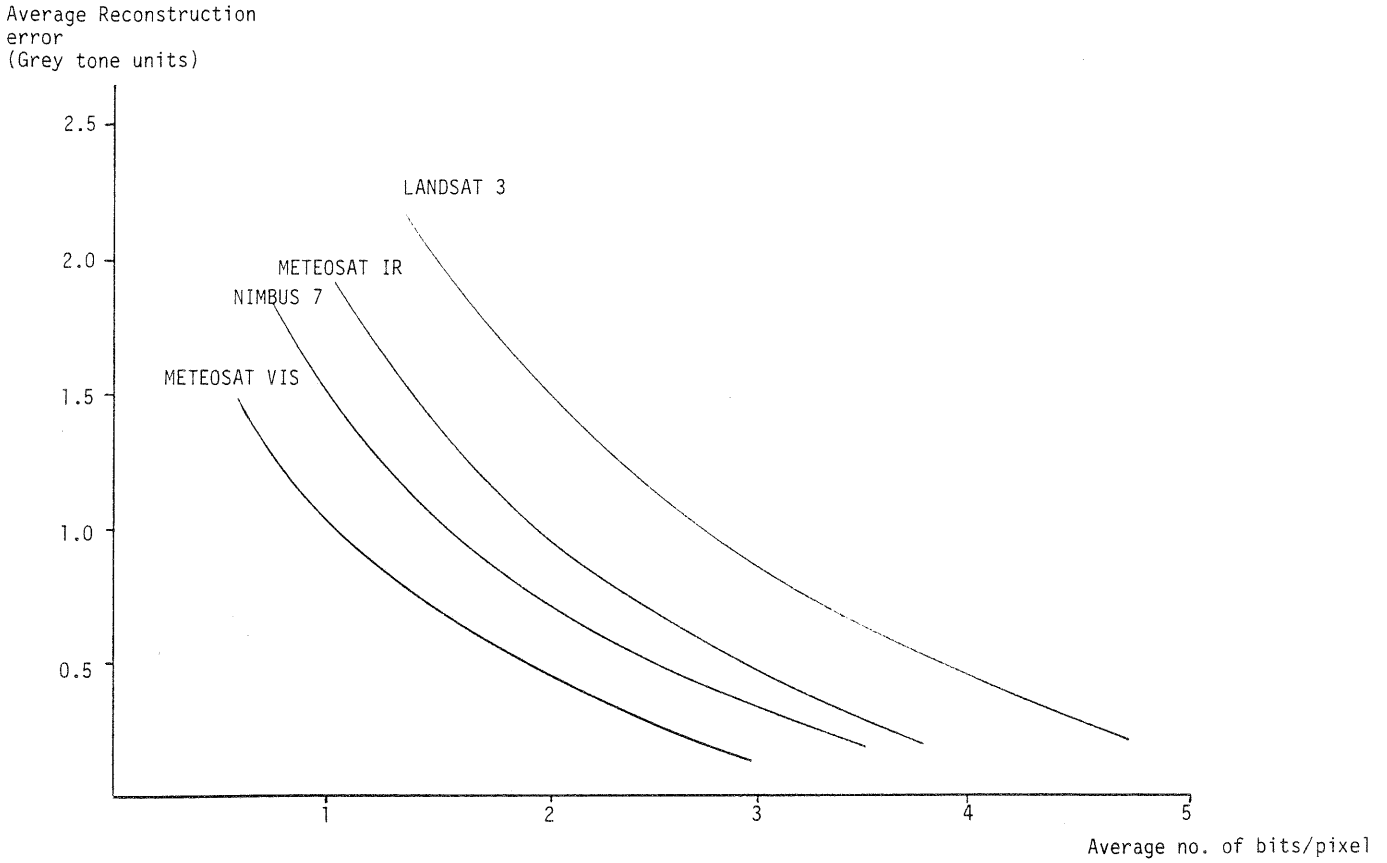

Figure 3 - Coding Performance on Various Earth Observation Satellite Image Data

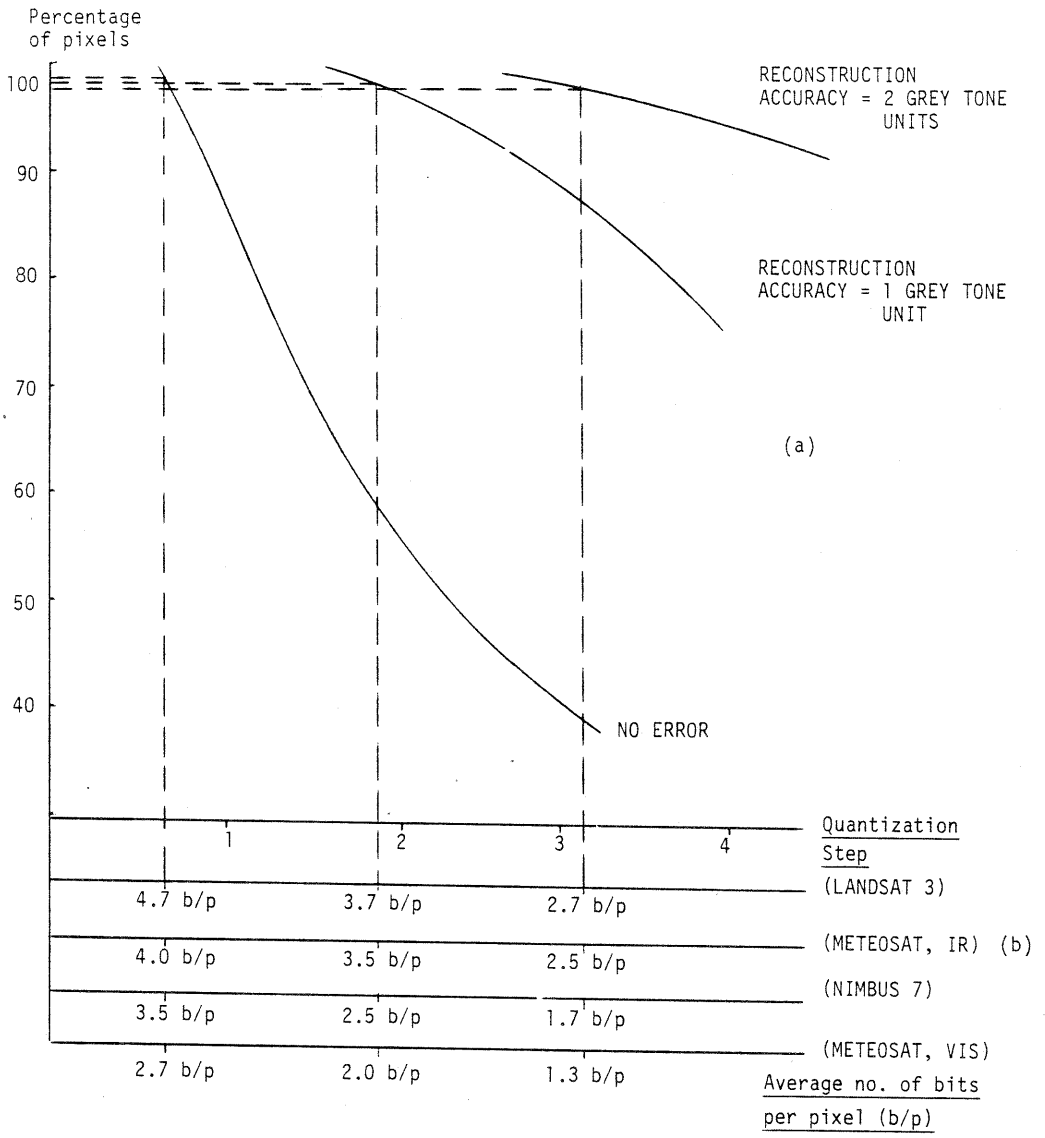

Figure 4 - Coding Performance versus tolerated Peak Error

Quant. Step Q / Data	0.8	1.7	3.4	6.8
LANDSAT 3	1 (2)	3 (3)	4 (7)	10 (14)
METEOSAT IR	1 (2	2 (3)	5 (7)	12 (14)
NIMBUS 7	1 (2)	2 (3)	5 (7)	14 (14)
METEOSAT VIS	1 (2)	3 (2)	5 (7)	9 (14)

Fig. 5 - Measured peak reconstruction error (grey tone unit levels)

(N.B. : In brackets: value derived from the theoretical expression).

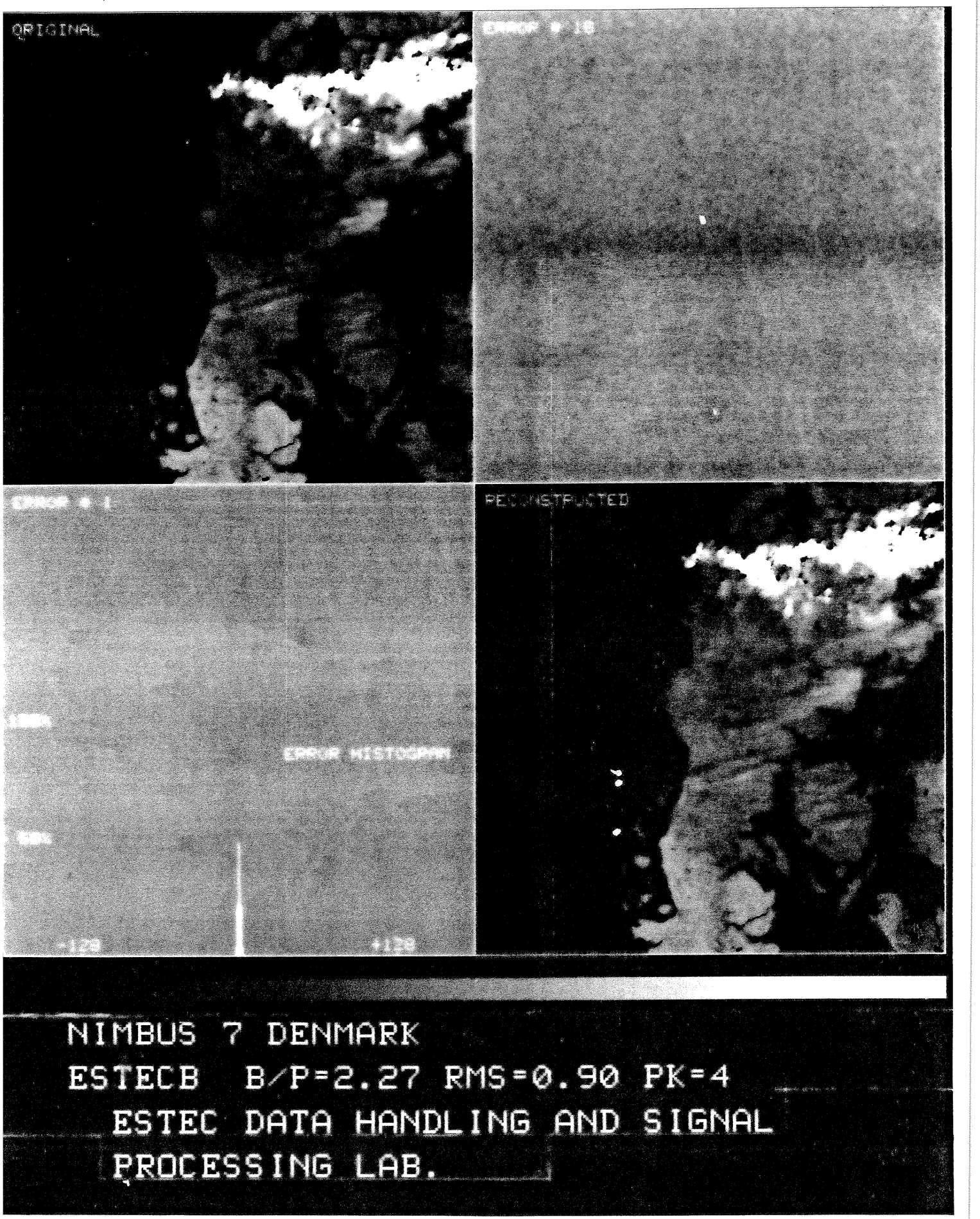
ORIGINAL
ERROR * 10
ERROR * 1
RECONSTRUCTED
ERROR HISTOGRAM
-128
+128
NIMBUS 7 DENMARK
ESTECB B/P=2.27 RMS=0.90 PK=4
ESTEC DATA HANDLING AND SIGNAL
PROCESSING LAB.

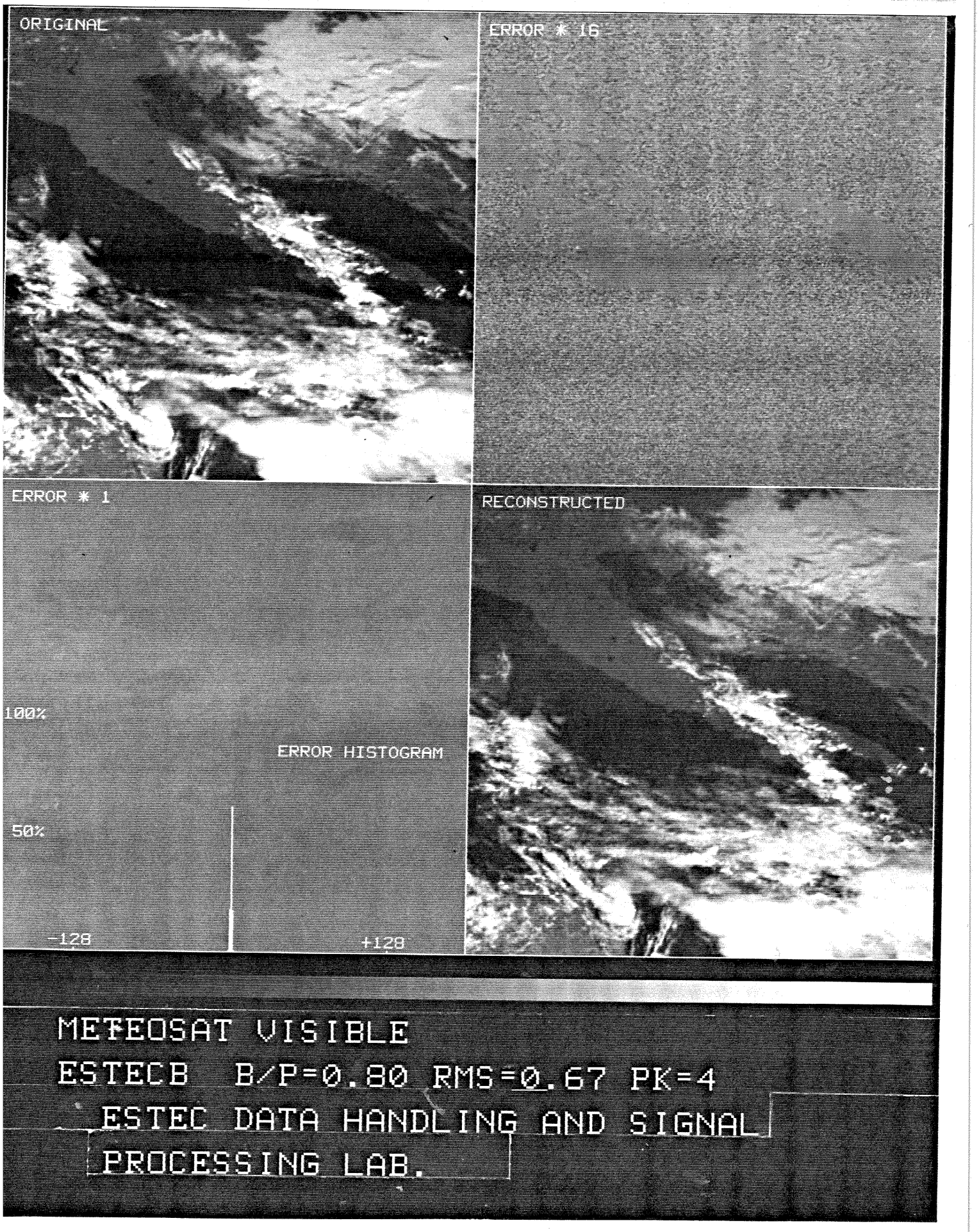
ORIGINAL
ERROR * 16
ERROR * 1
100%
ERROR HISTOGRAM
50%
-128
+128
RECONSTRUCTED
METEOSAT VISIBLE
ESTECB B/P=0.80 RMS=0.67 PK=4
ESTEC DATA HANDLING AND SIGNAL
PROCESSING LAB.

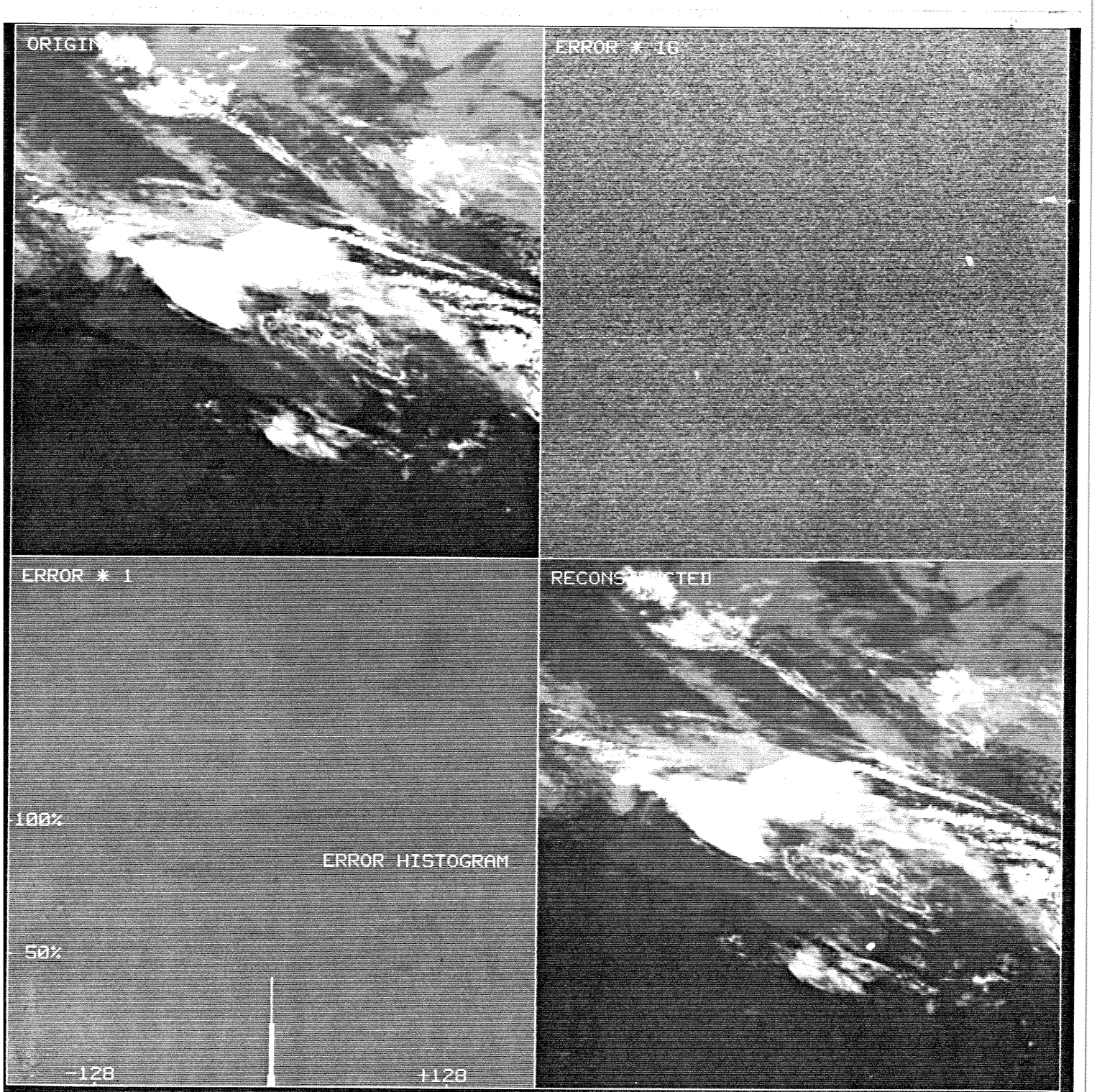
ORIGIN
ERROR * 16
ERROR * 1
100%
ERROR HISTOGRAM
50%
-128
+128
RECONS
METEOSAT INFRARED
ESTECB B/P=2.07 RMS=0.96 PK=4
ESTEC DATA HANDLING AND SIGNAL
PROCESSING LAB.

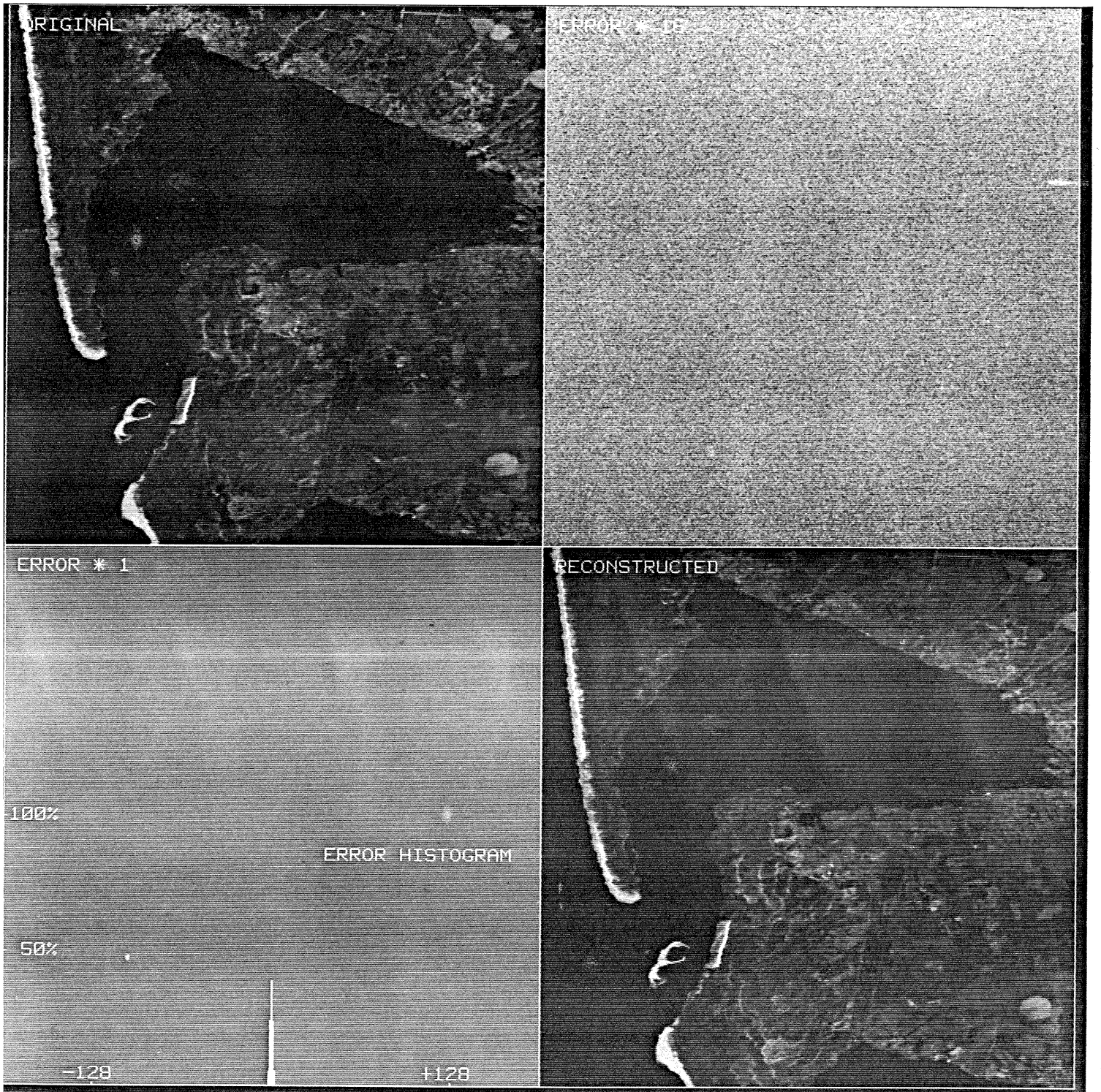
ORIGINAL
ERROR * 10
ERROR * 1
RECONSTRUCTED
100%
ERROR HISTOGRAM
50%
-128
+128
LANDSAT ARCACHON BAND 4
ESTECB B/P=2.86 RMS=1.02 PK=5
ESTEC DATA HANDLING AND SIGNAL
PROCESSING LAB.

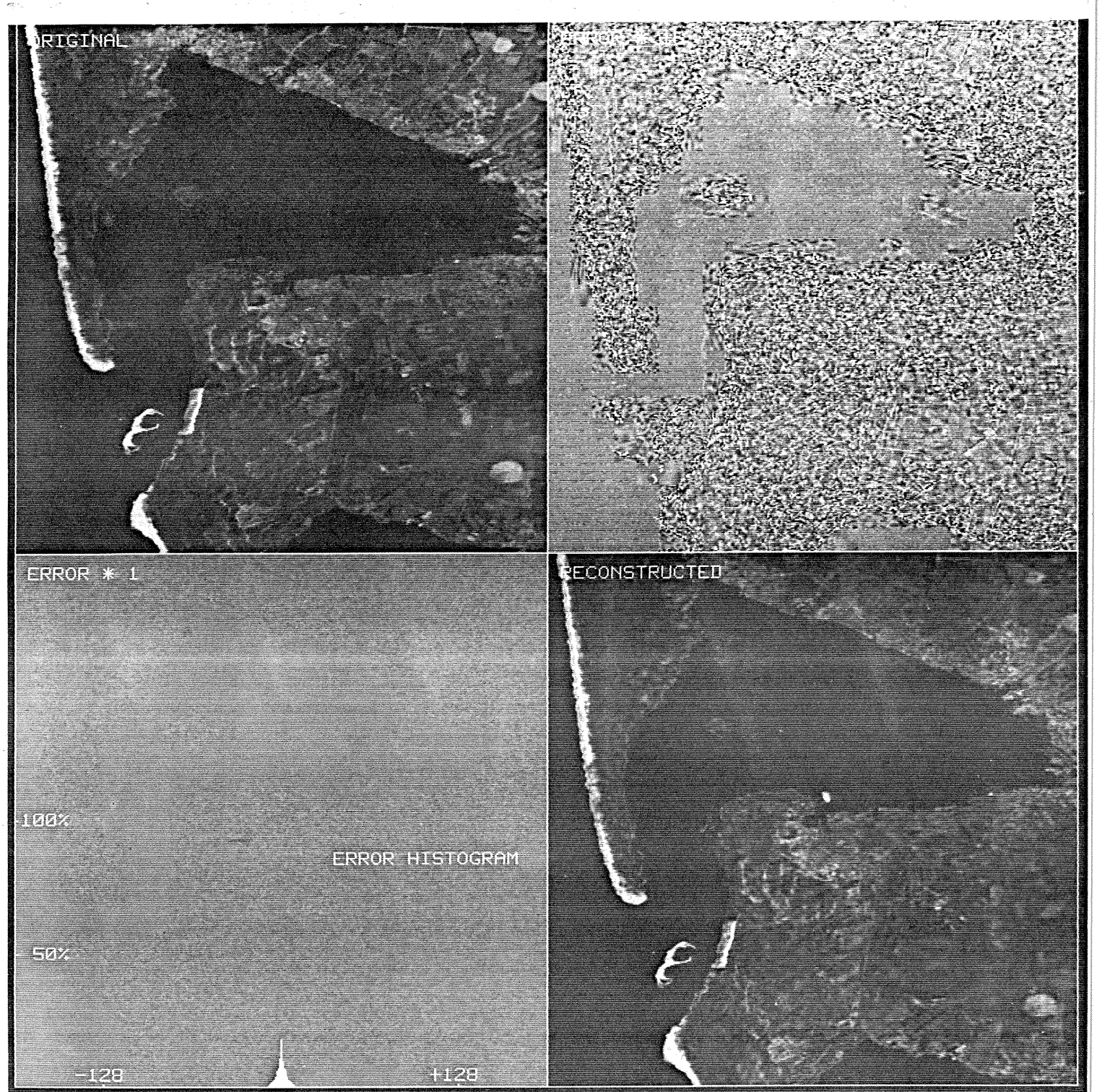

LANDSAT ARCACHON BAND 4
ESTECB B/P=0.54 RMS=4.41 PK=49
ESTEC DATA HANDLING AND SIGNAL PROCESSING LAB.